

Research on Engineering Structures & Materials



www.jresm.org

Research Article

Optimizing water-cement ratio for fly ash nano-silica mortar: Strength and microstructural insights

Mira Setiawati a, Anis Saggaff b, and Saloma *,c

Dept. of Civil Engineering, Faculty of Engineering, Sriwijaya University, Ogan Ilir, 30662, Indonesia

Article Info

Abstract

Article History:

Received 31 July 2025 Accepted 23 Nov 2025

Keywords:

Nano-silica; Fly ash; Mortar; Water to cement ratio; Compressive strength; Microstructure This study conducts a deeper analysis of mortar's mechanical and microstructural characteristics by examining the influence of nano-silica derived from fly ash on mortar's compressive strength and microstructure using the ratios of water-tocement (w/c) of 0.40, 0.45, and 0.485. Nano-silica was synthesized via the sol-gel method, yielding amorphous spherical particles ranging from 30 to 80 nm in size, with 98.37% SiO₂ content, as observed from SEM micrographs. XRD patterns revealed a broad peak at $2\theta \approx 22^{\circ}$, confirming the amorphous nature of the synthesized silica. FTIR spectra exhibited characteristic Si-O-Si and Si-OH vibrations at 1080 cm⁻¹ and 950 cm⁻¹, respectively, verifying the presence of silica networks. Mortar mixtures contained nano-silica ranging from 1%, 2%, 3% and 4% by cement weight and were tested after 28 days of curing. The highest compressive strength was achieved with 1% nano-silica at w/c = 0.40, showing more than a 29% increase compared to the control sample. Unlike prior studies, this work integrates compressive strength, SEM, XRD, and FTIR analyses in a single investigation of fly ash-derived nano-silica under varying w/c ratios. Additionally, XRD and FTIR analyses indicated increased C-S-H formation and hydration level, while SEM showed a denser matrix with fewer pores. The results highlight that the optimal nano-silica content improves mortar performance and promotes the sustainable use of industrial waste. Overall, nano-silica derived from fly ash effectively enhances the microstructure and mechanical performance of mortar by promoting C-S-H gel formation and densifying the interfacial transition zone. This study provides new insight into the potential of fly ash waste valorization for producing functional nanomaterials in sustainable cementitious systems.

© 2025 MIM Research Group. All rights reserved.

1. Introduction

Mortar is one of essential construction materials that primarily functions as a binding medium for bricks, concrete blocks, and other structural components. Its basic formulation typically comprises cement, sand, and water. With advances in material science and engineering, significant efforts have been made to enhance mortar performance, particularly in terms of mechanical strength, durability, and environmental sustainability. Additionally, compressive strength is widely recognized as a key parameter for evaluating mortar quality and structural reliability. This property is influenced by several factors, including the water–cement ratio, aggregate grading and distribution, and the incorporation of supplementary additives. Among these, the water–cement ratio (W/C) exerts a decisive influence, as it directly affects porosity and the quality of interparticle bonding within the hardened matrix. An increased W/C ratio generally results in higher water content, promoting pore formation and consequently reducing compressive strength.

In recent decades, the development of concrete and mortar technology has increasingly utilized innovative additives. One promising additive is nanomaterials, especially nano-silica. Nano-silica is

*Corresponding author: salomaunsri@gmail.com

^aorcid.org/0000-0001-6873-6418; ^borcid.org/0000-0002-7760-7797; ^corcid.org/0000-0003-4302-0282

DOI: http://dx.doi.org/10.17515/resm2025-1053ma0731rs

Res. Eng. Struct. Mat. Vol. x Iss. x (xxxx) xx-xx

characterized by its tiny particle size (generally <100 nm) [1] and high specific surface area, enabling it to fill micro-pores in the concrete matrix, improve the microstructure, react faster with cement hydration compounds, and improve its strength and durability [2-4]. An environmentally friendly source of n.ano-silica is fly ash, a by-product of coal combustion that shows great potential as a partial substitute for cement in mortar. Using fly ash as a source of nano-silica not only adds value to industrial waste but also supports the concept of waste-to-resource concept in the construction industry [5]. Various studies show that nano-silica synthesized from fly ash can significantly improve mortar performance. Fly ash contains a large amount of silica, making it a suitable raw material for making nano-silica through specific chemical processes such as sol-gel methods, precipitation, or alkali-acid extraction [6-8]. Previous studies demonstrated that nano-silica from fly ash can significantly improve the performance of mortar and concrete.

Using nano-silica from fly ash as an additive in mortar has positively affected its physical and mechanical properties. In general, the addition of nano-silica improves the compressive and tensile strength of mortar, refines pores microstructure by filling micro-cavities, and improves resistance to water and aggressive chemicals penetration [9-13]. This improvement is attributed to the pozzolanic reaction between nano-silica and calcium hydroxide (Ca(0H)₂), produced during cement hydration, which generates additional calcium silicate hydrate (C-S-H) compounds [14]. nano-silica can be used either as a dry powder or in colloidal form [15]. Colloidal nano-silica accelerates the hydration reaction, thereby improving the early strength development of TBNC [16]. Microstructural characterization has a crucial role in elucidating the mechanisms underlying material modification induced by the incorporation of nano-silica. X-ray diffraction (XRD) analysis is utilized to identify crystalline phases such as portlandite, quartz, and calcium silicate hydrate (C-S-H). Scanning electron microscopy (SEM) provides detailed insights into the topography and density of the mortar matrix, while Fourier-transform infrared spectroscopy (FTIR) detects functional groups associated with hydration products, including Si-O, Al-O, and OH bonds.

The observed improvements are believed to result primarily from two mechanisms: the filler effect of nanoparticles and the water-to-cement (w/c) ratio[15], which is a critical parameter in mortar mix design[16-17]. An excessively low w/c ratio may hinder hydration and reduce workability, whereas an excessively high ratio increases porosity and reduces compressive strength. Hence, assessing the interaction between nano-silica incorporation and the w/c ratio is essential for optimizing mortar performance. Moreover, utilizing fly ash as a secondary source of nano-silica provides additional advantages for environmental sustainability. This approach not only minimizes industrial waste but also reduces cement consumption, thereby lowering carbon emissions associated with cement production. Consequently, the application of nano-silica derived from fly ash in mortar systems contributes to enhanced material performance and advances the principles of sustainable construction and development. Furthermore, this research aims to:

- Examine the effect of nano-silica incorporation on mortar properties, particularly in improving mechanical performance and microstructural characteristics.
- Analyze the effect of the water-to-cement ratio (W/C) and the substitution of 1% to 4% nanosilica by weight of cement on the compressive strength of mortar, as a key indicator of mechanical strength.
- Investigate microstructural changes in mortars due to nano-silica substitution through material characterization using X-ray Diffraction (XRD) to identify crystalline phases, Scanning Electron Microscopy (SEM) to observe surface morphology and pore structure, and Fourier Transform Infrared Spectroscopy (FTIR) to identify chemical functional clusters formed during hydration.

Previous studies reporting the positive effect of nano-silica incorporation in concrete on mechanical strength and durability mostly focused on the effect of W/C ratio and various resources of fly ash synthesis. However, few studies have quantified the combined effect of nano-silica dosage and the w/c ratio on both hydration products and compressive strength using a multi-technique approach. This research addresses that gap by measuring mortar compressive strength and conducting characterization analysis using multiple analytical techniques, including X-ray Diffraction (XRD), Scanning Electron Microscopy (SEM), and Fourier Transform Infrared Spectroscopy (FTIR). This study provides a comprehensive explanation of how synthesized nano-

silica interacts with cement hydration compounds to improve mortar microstructures and mechanical performance. In other words, the novelty of this work lies in combining optimized inhouse synthesized nano-silica with systematic variations in the w/c ratio and deeper multitechnique microstructural characterization to provide a holistic view of how nano-silica interacts with cement hydration products to enhance mortar performance.

2. Materials and Method

2.1. Materials

The main materials used in this study are Portland cement type I, natural fine sand, clean water, and nano-silica derived from fly ash. The fine aggregate used in the mortar was sourced from Tanjung Raja, Ogan Ilir Regency.

2.2. Nano-Silica Derived from Fly Ash

Nano-silica was synthesized from fly ash through the sol-gel method [22]. The synthesis process began by sieving the material through a 200-mesh filter to ensure uniform particle size. The sieved material was leached with a $4.5~\rm M~HNO_3$ solution under varying liquid-to-solid (L/S) ratios of 1:15, combined with aging periods of 12 days. The mixture was magnetically stirred for 15 minutes at room temperature to ensure homogeneity and then filtered to separate the silica-rich filtrate from insoluble residues such as alumina and iron oxides. The filtrate was aged to form silica gel, which was washed with deionized water until a neutral pH was achieved. The resulting gel was ovendried at 120 °C to obtain amorphous silica powder and subsequently calcined to enhance purity. The synthesized nano-silica was characterized using XRD to confirm its amorphous nature, XRF to determine chemical purity, and SEM to observe particle morphology. The overall synthesis process is presented in Figure 1.

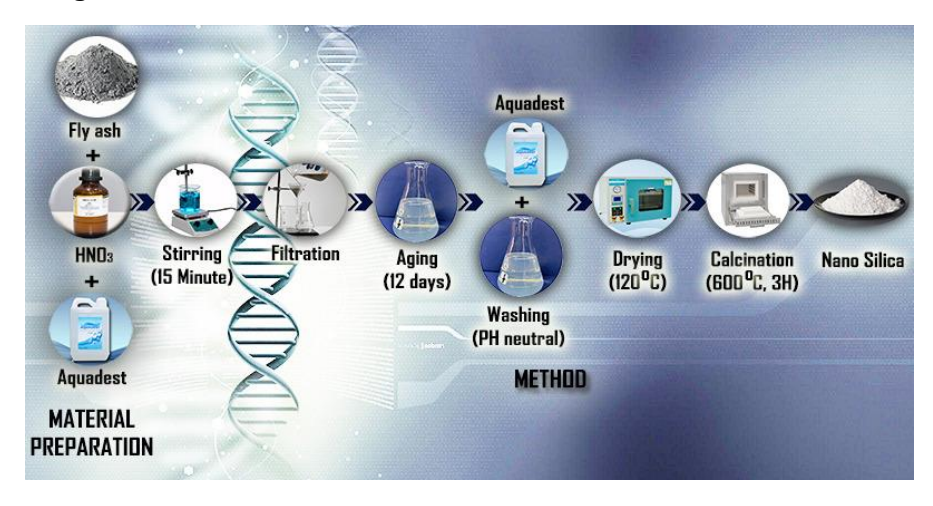


Fig 1. Schematic procedure of synthesis for fly ash

2.3. Mortar Mix Proportion

In this study, five mortar mixtures with different w/c ratios (0.4, 0.45 and 0.485) were produced to evaluate the impact of nano-silica derived from fly ash on compressive strength of mortar. The mixtures were designated as A, B1, B2, B3, and B4. Mixture A consisted of fine natural aggregate, cement, and water, while mixtures B1, B2, B3, and B4 contained varying nano-silica contents. Nano-silica was used to partially replace cement at 1%, 2%, 3%, and 4% by weight [11] . In the initial mixing step, the binder-to-sand ratio was maintained at 1:2.75, with w/c ratios of 0.4, 0.45, and 0.485. Cubes with size $50 \times 50 \times 50$ mm were prepared for compressive strength testing. Each mold was filled in two layers, with each layer compacted using four rounds of tamping, totaling 32 strokes, to ensure uniform filling and prevent segregation. After tamping, the mortar surface was allowed to slightly protrude above the mold, then leveled using the flat side of a trowel drawn once across the top and along the mold's length. Following molding, the specimens placed were in the

moist room for 24 hours. The mortar samples' compressive strength (CS) tests were determined after 28 days of curing. Table 1 illustrates the mixture proportions of the mortar specimens.

Table 1. Mixture proportions of mortar

No	w/c ratio	Sample	w/c	Cement	Fine aggregate	Nano-silica
		Code	(gr)	(gr)	(gr)	(gr)
1	0.4	A	244.80	612.00	1430	0
2	0.4	B1	244.80	601.58	1430	10.43
3	0.4	B2	244.80	591.15	1430	20.85
4	0.4	В3	244.80	580.72	1430	31.28
5	0.4	B4	244.80	570.30	1430	41.70
1	0.45	A	275.40	612,00	1430	0
2	0.45	B1	275.40	601.58	1430	10.43
3	0.45	B2	275.40	591.15	1430	20.85
4	0.45	В3	275.40	580.72	1430	31.28
_ 5	0.45	B4	275.40	570.30	1430	41.70
1	0.485	A	296.82	612,00	1430	0
2	0.485	B1	296.82	601.58	1430	10.43
3	0.485	B2	296.82	591.15	1430	20.85
4	0.485	В3	296.82	580.72	1430	31.28
_ 5	0.485	B4	296.82	570.30	1430	41.70

where; A is mortar mix without nano-silica, B refers to the mixes with various substitution proportions.

2.4. Compressive Strength Testing

The compressive strength test was conducted after 28 days using a universal compression testing machine in accordance with ASTM C109 standards. Six specimens were tested for each mix variation, and the average value was recorded as the representative strength. The 28-day period was selected as it is the standard reference for evaluating the final strength of cement-based materials. This test aimed to determine the effect of nano-silica addition and different water-to-cement ratios on mortar performance.

2.5. Characterization of Microstructures

Mortar microstructures were characterized using SEM to examine morphology, X-ray diffraction to identify and analyze crystalline phases, and FTIR to identify functional groups. Scanning electron microscopy with energy-dispersive X-ray (SEM/ EDX) type Phenom Pro Desktop was used to analyze the morphology and elemental compositions of mortar and silica. A Fourier Transform Infrared (FTIR) spectrum (Perkin-Elmer 2000) was obtained from pellets prepared by mixing the sample with spectroscopic-grade KBr at a mass ratio of 1:100 and analyzed over a wave number range of 4000–400 cm⁻¹. X-ray diffraction (XRD) patterns were recorded using a X-ray diffractometer (RIGAKU Miniflex 600 instrument) operated at 30 V and 10 mA, scanning diffraction angles from 10° to 80° (2θ) at a rate of 81 min⁻¹. Particle size distribution was measured by dynamic light scattering (DLS) at 25 °C with a dispersant refractive index of 1.3328 and viscosity of 0.8878 cP.

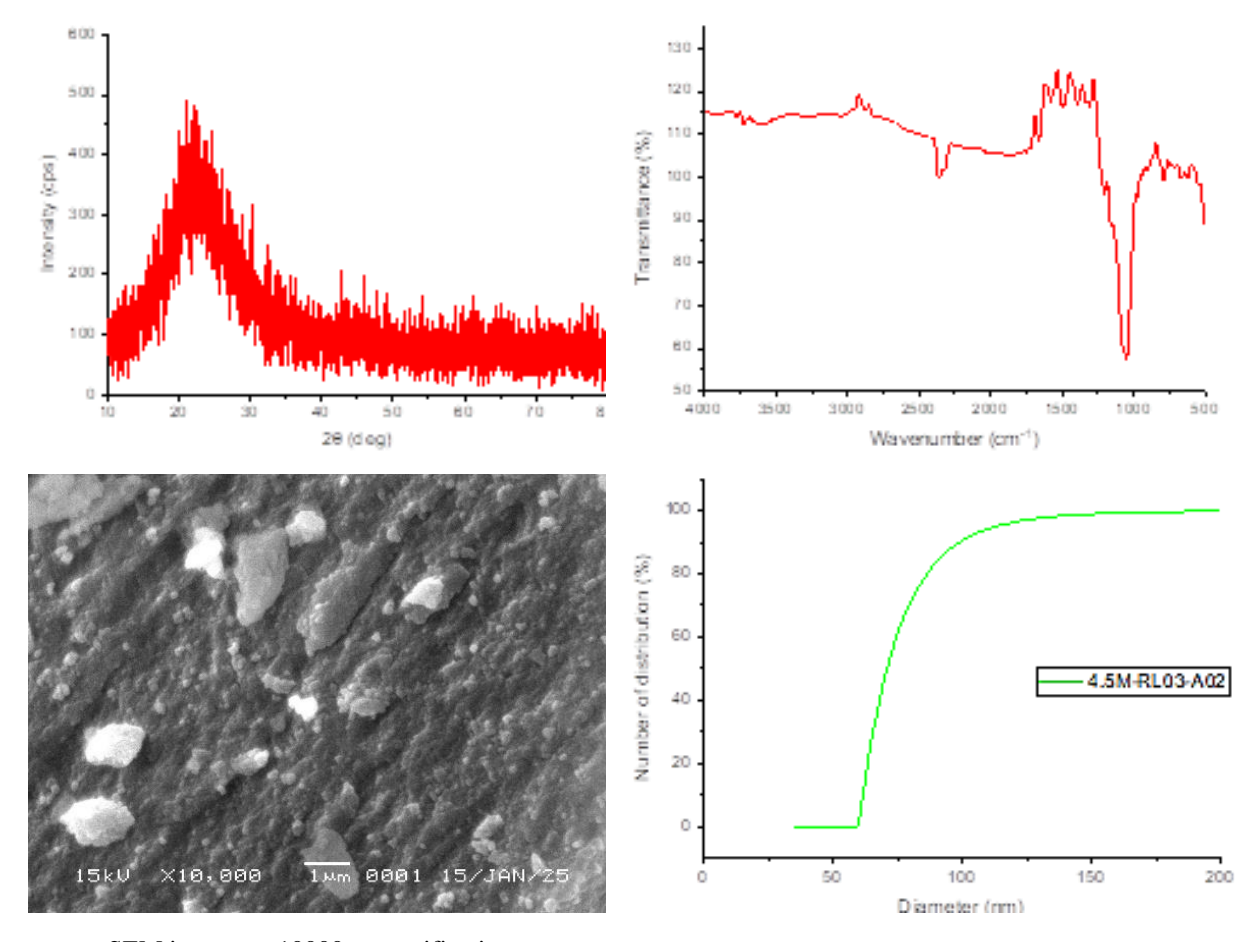
3. Results and Discussion

3.1. Characteristic of Nano-silica

The chemical composition of the synthesized nano-silica, measured using an XRF analytical device, is presented in Table 2, displaying a high nano-silica percentage of over 98%. While the X-Ray Diffraction (XRD) characterization results are shown in Fig. 2a. As illustrated, a broad and low-intensity peak appears at approximately $2\theta = 22^{\circ}$, a typical feature of amorphous SiO₂, indicating the amorphous nature of the material [19]. The moderate peak intensity (~520 cps) also confirms

the absence of long-range crystalline order. Area integration indicates that approximately 88-92 % of the material is amorphous, with no detectable quartz or cristobalite peaks. In other words, the absence of sharp crystalline peaks confirms that the silica structure has been successfully converted into an amorphous form signifying that the sol–gel synthesis has produced high-purity amorphous nano-silica (98.37 % SiO_2 from XRF) which is crucial for enhancing pozzolan reactivity in the mortar mixture.

Furthermore, the FTIR spectrum of the synthesized nano-silica (Fig. 2b) reveals distinct absorption characteristic of amorphous SiO_2 . A broad band centered near 3440 cm⁻¹ corresponds to O-H stretching vibrations of surface silanol groups and adsorbed moisture, while the shoulder at approximately 1630 cm^{-1} represents the bending mode of molecular water. The dominant peak at 1080 cm^{-1} , showing a $\sim 65 \%$ reduction in transmittance, is signaled to asymmetric Si-O-Si stretching within the silicate network, confirming extensive polymerization of SiO_4 tetrahedra. Additional absorptions at around 800 cm^{-1} (symmetric Si-O-Si) and 460 cm^{-1} (Si-O bending) further substantiate the presence of a non-crystalline silica framework, while the strong O-H relates to a hydroxyl-rich surface favorable for pozzolanic reactivity. These functional groups confirm the presence of amorphous silica structure with a high potential to form chemical bonds with the cement matrix. This aligns with research conducted by [23], which described similar FTIR spectra for extracted silica.



SEM images at 10000x magnification

Fig. 2. Characterization results of nano-silica

SEM images at 10000x magnification (figure 2c) showed that the synthesized nano-silica particles have irregular shapes and tend to form agglomerations, which may limit the dispersibility due to persistent clustering after processing. Detailed analysis also identifies nanometer-sized primary particles evenly distributed across the matrix. PSA results (figure 2d) showed a median hydrodynamic diameter (D50) of 70.8 nm, consistent with the primary particle size observed in the SEM images (<100 nm), indicating that most particles are in the nano size range [5,19.21,22] {Formatting Citation}. This distribution pattern indicates the successful synthesis of nano-silica

with dominant particle sizes below 100 nm, an important feature for reaching high surface area and enhanced reactivity [25]. The minor agglomerations observed in the SEM images are likely attributed to the drying process during sample preparation. The difference between SEM and PSA measurements occurs because PSA detects the hydrodynamic diameters of particles in suspension, accounting for solvation and particle interactions, where particle size measurement was performed at a 25°C using water (H_2O) as the dispersing medium. Water was selected for its inertness and optical stability, ensuring accurate particle dispersion analysis. The solvent's physical parameters included a refractive index of 1.3328 and a viscosity of 0.8878 cP, consistent with water properties at 25°C. The scattering intensity of 9380 cps indicated a stable particle suspension with sufficient signal strength for accurate particle size determination, while SEM reveals only the dry core size. These characterization findings confirm that the synthesized material corresponds to amorphous nano-silica with favorable particle size distribution, irregular morphology, and active functional groups. Such properties highlight its potential as an additive in mortar systems, contributing to enhanced strength, density, and microstructural performance.

Table 2. Chemical composition of nano-silica (%)

Sample		XRF Analysis Results (%)							
Sample	SiO ₂	Fe_2O_3	Ca0	TiO ₂	Al_2O_3	Cr_2O_3	MgO	Na ₂ O	K ₂ O
Nano-silica	98.387	0.052	0.535	0.075	0.589	0.013	0.144	0.206	< 0.010

3.2. Compressive Strength Test Results

The slump, compressive strength and standard deviation of the mortar are illustrated in Tables 3-5. The compressive strength data showed a significant increase in samples with 1% - 4% nanosilica substitution. The range of nano-silica percentage was determined based on effectiveness and efficiency aspects from preliminary tests and previous studies [10,12-13]. In this work, the highest compressive strength was recorded at 1% nano-silica with a w/c ratio of 0.4, reaching 35.07 MPa.

Table 3. The compressive strength of mortar

w/c ratio	Average of the compressive strength (Mpa)					
	A	B1	B2	В3	B4	
0.4	27.17	35.07	31.98	27.27	25.68	
0.45	26.12	33.51	29.45	27.17	24.97	
0.485	25.80	30.88	26.99	25.54	23.80	

The slump test results revealed that the slump value of the mortar increased with a higher water-to-cement (w/c) ratio but decreased with increasing nano-silica substitution. For plain mortar, the slump rose from 42 mm at w/c = 0.40 to 68 mm at w/c = 0.485, indicating improved workability due to higher water content. However, the inclusion of 1–4% nano-silica caused a consistent reduction in slump at each w/c ratio. For example, at w/c = 0.45, the slump decreased from 53 mm to 50 mm, 45 mm, 40 mm, and 38 mm for 1%, 2%, 3%, and 4% nano-silica substitution, respectively.

Table 4. Slump test of mortar

w/c ratio	Slump Test (mm)					
	A	B1	B2	В3	B4	
0.4	42	38	32	30	27	
0.45	53	50	45	40	38	
0.485	68	61	60	56	50	

This reduction in slump is primarily attributed to the high specific surface area and hydrophilic nature of nano-silica particles, which absorb part of the mixing water and decrease the amount of free water available for lubrication in the mixture. Furthermore, nano-silica particles enhance early hydration reactions and increase the viscosity of fresh mortar. In order to evaluate the effect of moisture content (40%, 45%, 48.5%) and mixture type (B1, B2, B3, B4) on the compressive strength of the mortar, a two-way ANOVA analysis without replication was performed. In this

study, the normality and homogeneity of variances were not specifically tested. The calculation results are presented in Table 6, showing the critical F, p-value, and F values for each factor. The analysis indicates that both moisture content factor and the mixture type significantly influence the compressive strength of the mortar. For the moisture content factor, the F value (13.67) exceeds the critical F (4.46), with a p-value of 0.00 (< 0.05). This shows that changes in moisture content significantly influence the compressive strength of the mortar. In general, increased moisture content tends to reduce compressive strength, consistent with the theory that a higher water-cement ratio results in greater porosity and lower strength

Table 5. The Standard Deviation of mortar

w/c ratio	Standard Deviation of mortar sample						
	A	B1	B2	В3	B4		
0.4	1,717256	2,115716	1,583217	2,295192	0,999455		
0.45	1,982225	1,806671	2,410744	1,958362	3,377973		
0.485	1,546536	1,584373	0,987413	1,52422	2,685088		

Table 6. Output for two-factor ANOVA analysis for mortar (MPa)

			· <i>y</i>	(')		
Source of Variation	SS	df	MS	F	P-value	F crit
Rows	20,22	2	10,11	13,67	0,00	4,46
Columns	129,88	4	32,47	43,91	0,00	3,84
Error	5,92	8	0,74			
Total	156,01	14				

The mixed-type factor also had a very significant influence, with F = 43.91 greater than the critical F = 3.84, and p-value = 0.00 (< 0.05). This indicates that differences in material composition among mixtures (B1-B4) significantly affected the resulting compressive strength. Based on average values, B1 mixture showed the highest compressive strength (33.15 MPa), while B4 produced the lowest compressive strength (24.82 MPa). These variations may be attributed to differences in fine aggregates, additives types, or workability that affect the mortar's density after hardening. The error value was relatively small (SS = 5.92, MS = 0.74), indicating that the variation in the test data remained within reasonable limits and that the results were consistent between replications. The total data variation was 156.01, with the largest proportion attributed to the influence of mixture factors (about 83% of the total SS). Thus, the results of this two-way ANOVA without replication confirm that both moisture content and mixture type significantly influence the compressive strength of mortar. In addition, the mixture type factor contributes to a more dominant variation than moisture content. Despite having limited view regarding mechanical performance, the findings of this 28-day compressive strength study align with the basic principle of concrete technology that optimizing material composition has a greater influence on strength than variations in moisture content in a limited range.

Figure 3 presents the compressive strength test results along with standard deviation of the mortar. It demonstrates that incorporating the additive markedly affected the samples' mechanical properties. The control specimen reached an average compressive strength of 25–27 MPa. At 1% nano-silica, the compressive strength peaked, notably in B1, reaching nearly 35 MPa. This improvement is attributed to nano-silica, filling micro-pores, refining the microstructure, and intensifying the pozzolanic reaction, thereby generating more C-S-H gel.

When the nano-silica dosage exceeded 1%, compressive strength progressively decreased. At 2% nano-silica, compressive strength ranged from 26 to 31 MPa and declined further at 3% and 4%, approaching or falling below the control value. This reduction is attributed to particle agglomeration, insufficient dispersion, and increased water demand, which reduce the density of the cement matrix and weaken interfacial bonding. The results demonstrate that a 1% additive dosage maximizes compressive strength, while higher dosages do not provide further improvement and instead reduce strength. These findings highlight the importance of identifying the optimal nanomaterial content to achieve the desired performance in mortar.

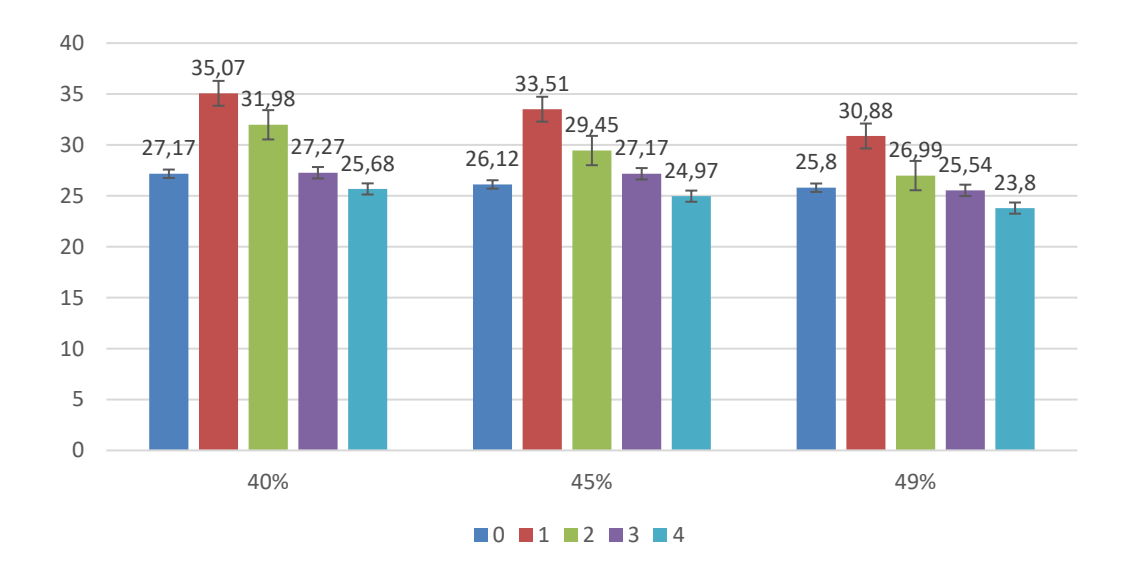
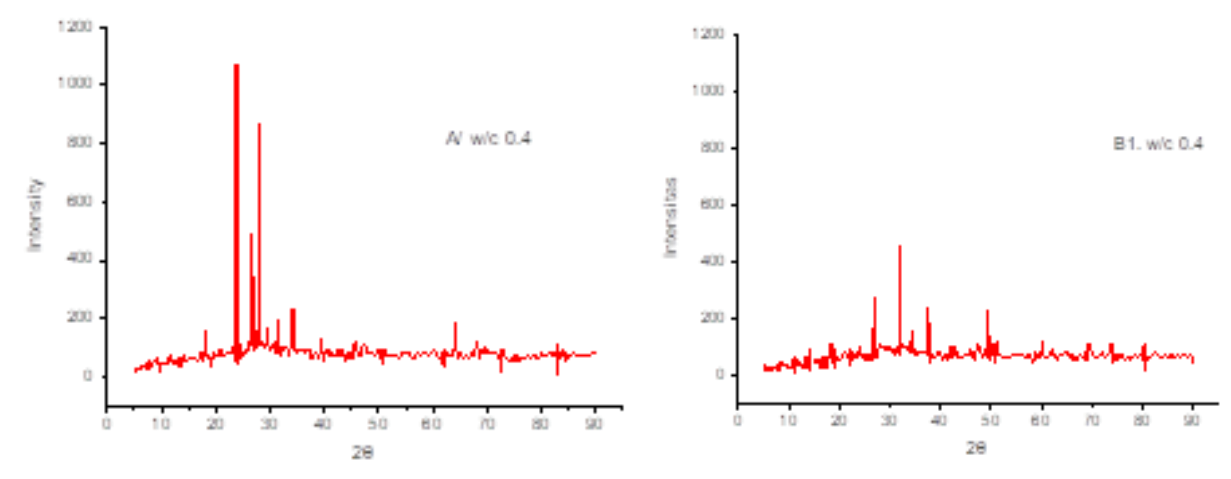


Fig. 3. Compressive strength of mortar

This work aligns with previous studies [16], which found that the enhancement of compressive strength continued as the CNS concentration increased up to 1% and slightly reduced at 2% and 3%. The decrease in CS may be attributed to particle separation due to excess nanoparticles or agglomeration caused by poor dispersion, which affects the pore structure of the concrete and decreases its strength. Furthermore [27], demonstrated that carefully controlled nanoparticle additions can enhance the early-age strength development of cement mortar without significantly altering its density or ultrasonic properties, making them promising additives for sustainable, high-performance construction materials. This finding also aligns with other studies, which reported that higher nano-silica content may be less effective due to particle agglomeration that reduces the workability of the concrete mixture [28].

3.3. XRD Test Result

Figure 4 shows X-ray diffraction (XRD) patterns of six mortar samples. The XRD analysis showed a decrease in the relative intensity of the portlandite (Ca(OH)₂) peaks at $2\theta \approx 18^\circ$ and 34° in mortars containing nano-silica, compared to the control mortar. The intensity ratio of portlandite to quartz, used as an inert reference phase, decreased consistently with increasing nano-silica content, indicating a pozzolanic reaction between amorphous Ca(OH)₂ and SiO₂ in nano-silica. At the same time, a broad hump appeared in the range of $28-34^\circ$, which is characteristic of amorphous C–S–H. According to [29], the high surface area of NS facilitated the formation of new C–S–H bonds, thereby enhancing mortar strength. This confirms that nano-silica substitution not only consumes portlandite but also accelerates the formation of C–S–H, the main hydration product acting as the strength contributor.



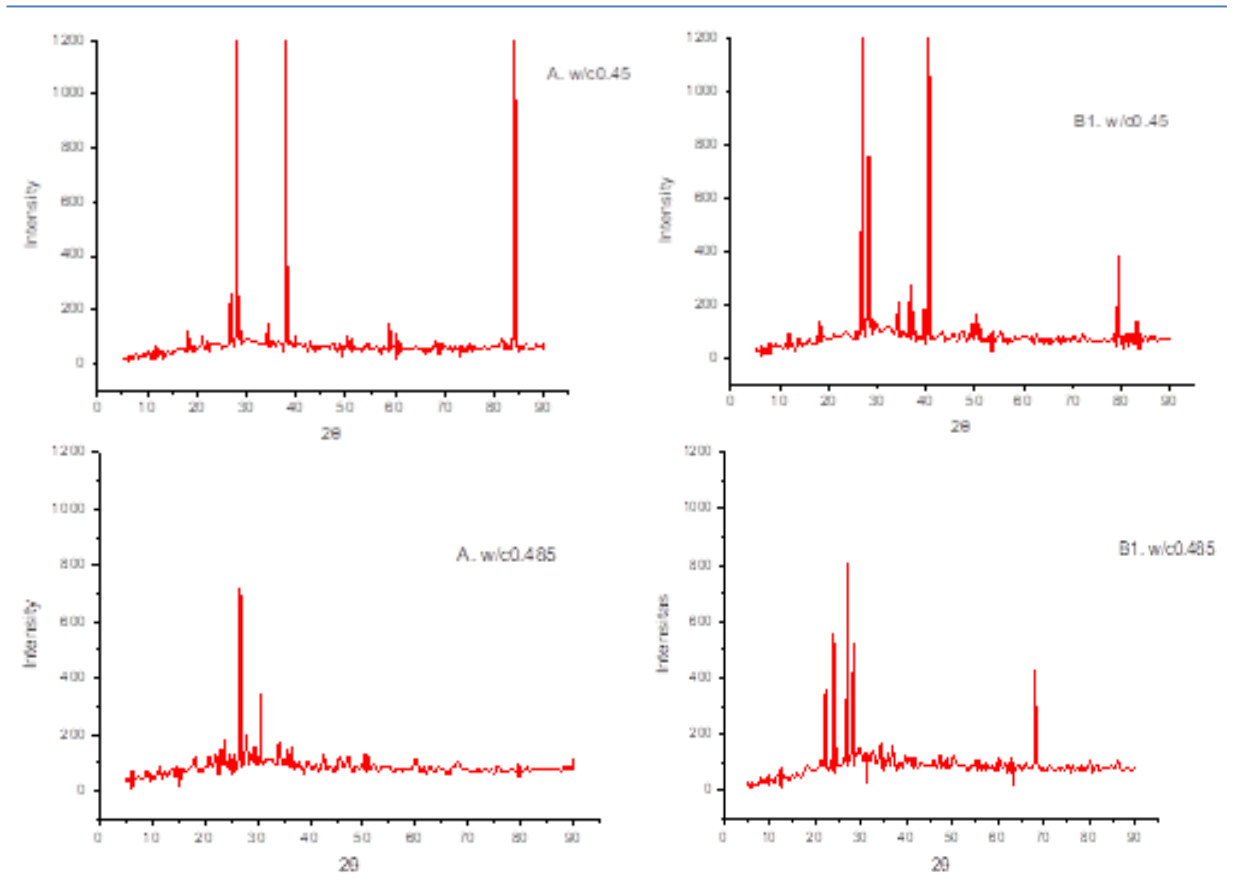


Fig. 4. XRD mortar pattern

Thus, the increase in compressive strength in mortars with nano-silica is mainly due to the pozzolanic mechanism, namely the consumption of Ca(OH)₂ and the increased C-S-H formation, which improve the matrix microstructure and reduce porosity. The compressive strength test results show that the addition of nano-silica consistently increases strength across water-tocement ratio. Overall, at every w/c ratio, the 1% nano-silica composition produced the highest value, while higher nano-silica content led to a decrease. This pattern aligns with the XRD results, which show a decreased portlandite peak intensity and a more pronounced amorphous C-S-H hump at 1% nano-silica, indicating the most efficient pozzolanic reaction. At 2% nano-silica, portlandite consumption remains evident but less significant by 1%, whereas at 3-4% the portlandite intensity stabilizes or slightly increases, corresponding with decreased compressive strength due to particle agglomeration and reduced reaction effectiveness. This correlation confirms that maximum strength is achieved when the portlandite consumption and C-S-H formation occur at approximately 1% nano-silica addition by cement mass. Furthermore, X-ray Diffraction (XRD) analysis showed that the nano-silica substitution derived from fly ash affected the composition of the hydrate phase in the mortar. The mixture containing 1% nano-silica and a w/c of 0.40 showed a decrease in the peak intensity of calcium hydroxide (Ca(OH)₂), while the peak associated with calcium silicate hydrate (C-S-H) increased, indicating a pozzolan reaction. This phenomena is attributed to the reaction between nano-silica and Ca(OH)₂ during hydration, resulting in additional C-S-H formation that increases strength and density of the microstructure, as depicted in the following reaction:

$$SiO_2(nano) + Ca(OH)_2 + H_2O \rightarrow C - S - H$$
 (1)

Based on the above reaction, the hydration mechanism begins with nano-silica from fly ash entering the hydration system and acting as highly reactive amorphous SiO_2 . It serves as a nucleation site that consumes $Ca(OH)_2$ through pozzolanic reactions to produce secondary C–S–H [18]. Although this process may reduce porosity, it increases the compressive strength of the mortar.

3.4. FT-IR Test Results

The FTIR test was performed using certified reference materials and known silica mineral samples, following the manufacturer's recommended procedures. The FTIR spectrum showed a shift in the Si-O-Si absorption band at around 1000-1100 cm-1 in samples containing nano-silica, indicating formation of more structured hydrated silicates (Fig. 5).

The intensity of the OH band also changed, indicating the interaction of nano-silica with water coordinated in the matrix. This finding aligns with XRD pattern analysis, which explains the increase in mechanical strength, especially in terms of chemical bonding in the mortar microstructure. The FTIR spectrum depicts the response of the chemical functional groups of each mortar sample in the wavenumber range of 4000–500 cm⁻¹. All samples, both the control (A) and the 1% nano-silica substitution (B1), showed similar absorption patterns, with some differences in intensity and peak sharpness reflecting changes in chemical structure due to the addition of nano-silica.

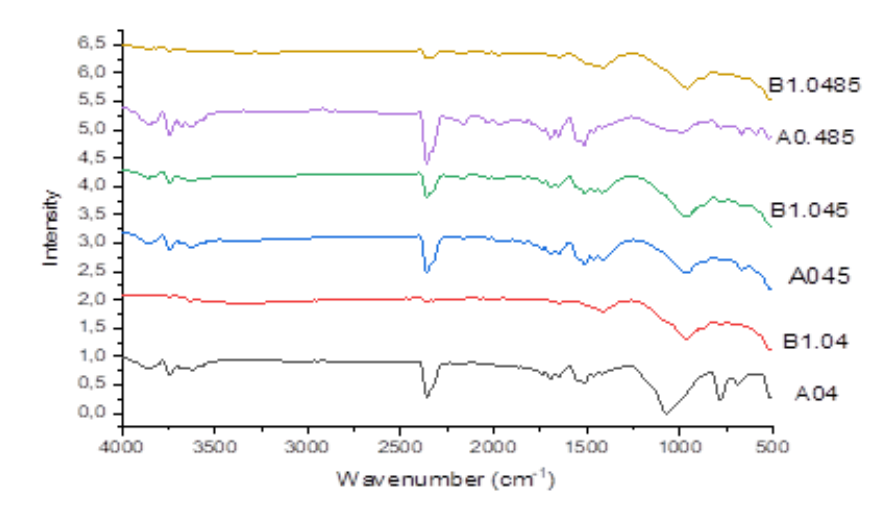


Fig. 5. Spectrum FT-IR mortar specimen

Table 5 presents the summary of FTIR bands, assignments, dominant samples, and implications for mortar control (A) and mortar with nano-silica substitution. The strong absorption band around 3400 cm⁻¹ corresponds to the stretching vibration of the -OH group, originating from bound water and hydroxyl groups in cement hydrate structures such as C-S-H (Calcium Silicate Hydrate) and ettringite. This peak appears slightly more intense in samples with nano-silica addition, suggesting increased bound water associated with the formation of more hydration phases. While having indication of acceptable reproducibility and data reliability of ANOVA with small error value (SS = 5.92, MS = 0.74), this study also acknowledged that there was experimental uncertainty.

The FTIR results showing increased intensity of the silanol (~960 cm⁻¹) and 0-H (3200-3500 cm⁻¹) bands in samples with nano-silica align with the XRD findings, where the diffraction pattern is dominated by broad amorphous silica peaks. This confirms that the material formed is amorphous, with an imperfect level of silica tissue condensation, leaving reactive silanol groups. This trend is reinforced by SEM results, which show a porous morphology with nano-micro sized particles and irregular agglomeration. The porous structure and the presence of active silanol groups simultaneously increase the specific surface area and chemical reactivity of the material. Thus, the correlation among FTIR, XRD, and SEM suggests that nano-silica not only alters the chemical composition (increased silanol groups) but also influences structural regularity (amorphous phase) and micro texture (porous morphology), thereby improving the reactivity potential of fly ash-based nano-silica.

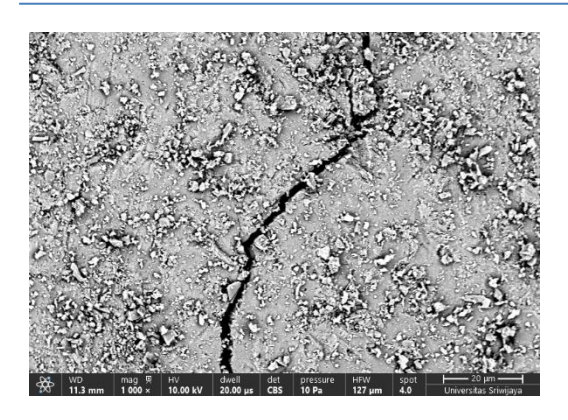
Table 5. Summary of FTIR bands, assignments, dominant samples, and implications

Wavenumber (cm ⁻¹)	Assignment	Dominant sample	Interpretive implications
3400-3200 (Wide)	Strain O–H (silanol, adsorbed water)	More clearly on B1.04, B2.045	Increased OH → indicates more silanol/water bound groups → surface area and higher surface reactivity
~1630	Bending H-O-H (dissorbed water)	Stronger on B1.04, B2.045	Higher water content → open pore structure and more hydrophilic material
1100-1000	Si-O-Si asymmetric stretching	All samples, main tape	Indicates a silica skeleton is formed; Position shifts may reflect the degree of tissue polymerization
~960	Si-OH stretching / Si- O-Ca (silanol, C-S-H)	More clearly on B1.04, B2.045	Increased intensity of this band → more active silanol groups → higher chemical reactivity and lower silica condensation
~800	Si-O-Si symmetric stretching	All samples	Indicates the presence of tetrahedral SiO ₄ → the stability of the silica base structure is maintained
1450 & 875	CO_3^{2-} (carbonate, from CO_2 exposure)	Moderate intensity in all samples	The presence of carbonation → can reduce the purity of silica, but it also indicates interaction with the environment
500-470	Si-0 / Al-0-Si Bending (aluminosilicate)	All samples	Demonstrated the contribution of fly ash (aluminosilicate) → indication of the Si–Al mixture in tissues

3.5. SEM Test Results

Figure 6-7 presents the SEM-EDX Micrographs of control mortar (A0.4) and mortar substituted with 1% nano-silica (B1.04), respectively. Figure 6 shows a relatively porous and non-homogeneous surface morphology, with microcracks distributed throughout the observed area. These cracks indicate internal stresses that may result from autogenic shrinkage, moisture differences, or imbalances in the hydration process. The accompanying EDX spectrum displays the dominant peaks of oxygen (O) and silicon (Si), along with significant signals of calcium (Ca), aluminum (Al), sodium (Na), and magnesium (Mg), elements typically found in cement hydration phase. The high Si/O ratio confirms the formation of hydrated silicate phases, while the presence of Ca indicates the contribution of hydration products such as calcium silicate hydrate (C–S–H) and possible portlandite residues (Ca(OH)₂).

In contrast, Fig. 7 presents the SEM-EDX micrographs of mortar substituted with 1% nano-silica (B1.04). It features a denser and more compact surface, with a texture dominated by smooth layers and clusters of bound particles, indicating further hydration. This area has lower porosity, which microstructurally implies increased mechanical resistance. The EDX spectrum exhibits 0, Si, and Ca peaks with relatively balanced intensity, indicating a more uniform formation of C–S–H and higher consumption of $Ca(OH)_2$ through pozzolanic reactions. The combination of morphological and elemental information suggests that a more complete hydration process contributes to crack reduction and increased matrix density, thereby increasing the mortar's compressive strength and durability. This suggests that using 4.5 M HNO $_3$ and 12-day aging likely produces chemically active nano-silica that disperses effectively within the mortar system.



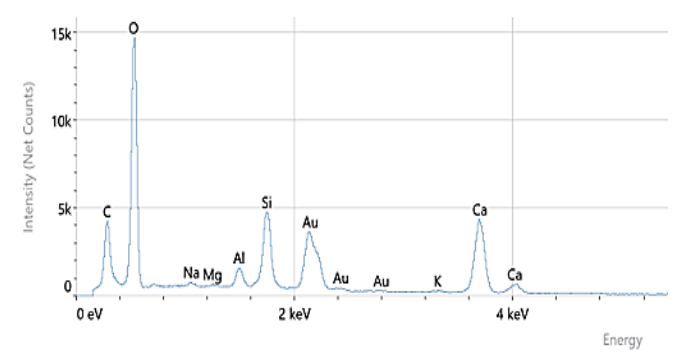
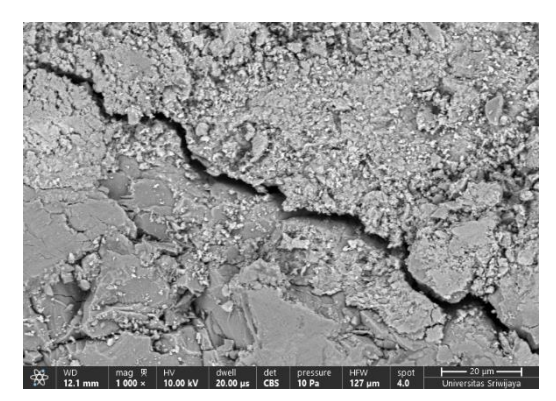


Fig. 6. SEM-EDX Micrographs of mortar specimen with w/c of 0.4



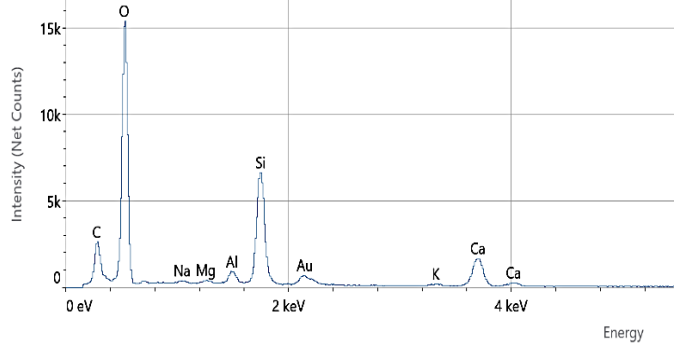


Fig. 7. SEM-EDX Micrographs of mortar specimen with partial substitution nano-silica

Scanning Electron Microscopy (SEM) results support this finding, showing that mortar with nanosilica shows a denser matrix structure and a smaller, homogeneous pore distribution than the control mortar. At the optimum 1% substitution, capillary pores are almost covered with C–S–H gel and uniformly dispersed nano-silica particles. Conversely, at nano-silica levels above 1%, particle agglomeration occurs, forming local cavities that may act as structural weak points.

The observation on the relationship amongst strength trend (optimum at 1 %), microstructural evidence, and slump values can also be clarified. The optimum compressive strength obtained at 1% nano-silica addition (35.07 MPa at w/c = 0.40) is closely associated with the microstructural densification evident in the SEM micrographs (Fig. 7), which display a compact matrix with markedly reduced porosity resulting from enhanced C–S–H gel formation. Meanwhile, the concurrent decline in slump values with increasing nano-silica content (Table 4) informing that the nanoparticles absorbed free water and refined the pore network, thereby improving packing density and mechanical integrity at low dosages. At higher substitution levels (>1%), particle agglomeration and elevated water demand adversely affected workability and hindered strength development.

5. Conclusions

Based on the findings of this study, the following conclusions can be drawn:

• The incorporation of fly ash–derived nano-silica significantly influences the mechanical and microstructural properties of mortar, although this study was limited to a single curing age and did not assess durability. Compressive strength testing demonstrated that, within the selected nano-silica and W/C ranges, the optimum nano-silica dosage of 1% combined with a W/C ratio of 0.40 yielded a maximum compressive strength of 35.07 MPa—an increase over 29% compared to the control mix. This improvement is primarily attributed to the dual role of nano-silica as a pozzolanic reactant and micro filler, which promotes the consumption of Ca(OH)₂ from cement hydration to form additional C–S–H gel while filling micro-pores, producing a denser and more homogeneous matrix.

- The 29% increase in mortar compressive strength at a w/c ratio of 0.40 suggests the potential to reduce cement content in the mixture by 27–40%. Determining the exact replacement level requires dedicated mix trials with incremental cement reductions, which are recommended as a key focus for future research.
- Mechanical testing and microstructural characterization confirm that the strength gain in mortar with 1% nano-silica at a W/C ratio of 0.40 arises from two principal mechanisms: (i) the filler effect, which reduces porosity by blocking capillary voids, and (ii) the pozzolanic reaction, which generates additional C–S–H phases, enhancing matrix density and strength. In contrast, higher nano-silica dosages reduced compressive strength, largely due to particle agglomeration creating weak zones and disrupting matrix integrity. These findings underscore that the effective application of fly ash–derived nano-silica in mortar requires both an optimized dosage and a suitable W/C ratio to ensure adequate particle dispersion.
- XRD analysis showed a decrease in portlandite peak intensity and a corresponding increase in C–S–H phase development in samples containing 1% nano-silica, confirming an enhanced pozzolanic reaction. FTIR spectra supported this observation, showing a shift in the Si–O–Si absorption band and increased –OH band intensity, reflecting more polymerized silicate networks and a greater abundance of hydrate phases. SEM micrographs corroborated these results, illustrating reduced porosity, more uniform particle dispersion, and improved pasteaggregate interfacial bonding in the 1% nano-silica mix compared to the control. In contrast, excessive nano-silica incorporation (>1%) negatively impacted compressive strength, due to agglomeration effects, elevated water demand, and reduced pozzolanic efficiency.
- The indication of 28-day compressive strength study may provide a limited view of mechanical performance; therefore, future research could be suggested to include early-age (3 and 7 days) and long-term (56 and 90 days) measurements to get better insight regarding the pattern of strength development pattern and pozzolanic kinetic reaction between nanosilica and cement hydration products.
- Beyond mechanical and microstructural improvements, this study highlights the sustainability potential of utilizing fly ash as a source of nano-silica. This approach reduces cement consumption, mitigates industrial waste, and lowers carbon emissions, offering both environmental and economic advantages for the construction industry.
- In addition to compressive strength, durability is crucial for long-term performance. This study did not include durability tests; therefore, future research focusing on water absorption or sorptivity is recommended to strengthen the findings and support the material's practical application.

Acknowledgement

The authors thank to The Department of Civil Engineering, Faculty of Engineering, Sriwijaya University, for providing the necessary facilities and support for this research. We would also like to thank the instructors in the laboratory who have assisted with its implementation.

References

- [1] Hameed MH, Abbas ZK, Al-Ahmed AH. Fresh and hardened properties of nano self-compacting concrete with micro and nano silica. IOP Conf Ser Mater Sci Eng. 2020;671. https://doi.org/10.1088/1757-899X/671/1/012079
- [2] Namvar M, Mahinroosta M, Allahverdi A. Highly efficient green synthesis of highly pure microporous nanosilica from silicomanganese slag. Ceram Int. 2021;47:2222-9. https://doi.org/10.1016/j.ceramint.2020.09.062
- [3] Purnomo CW, Wirawan SK, Hinode H. The utilization of bagasse fly ash for mesoporous silica synthesis. IOP Conf Ser Mater Sci Eng. 2019;543:1-7. https://doi.org/10.1088/1757-899X/543/1/012040
- [4] Udaibah W, Mulyatun, Farikha GP, Monica T. Synthesis fibrous silica from rice husk ash: Its opportunities and challenges. IOP Conf Ser Earth Environ Sci. 2021;796. https://doi.org/10.1088/1742-6596/1796/1/012109
- [5] Kamara S, Foday EH Jr, Wang W. A review on the utilization and environmental concerns of coal fly ash. Am J Chem Pharm. 2023;2:53-65. https://doi.org/10.54536/ajcp.v2i2.1609
- [6] Yadav VK, Fulekar MH. Green synthesis and characterization of amorphous silica nanoparticles from fly ash. Mater Today Proc. 2019;8:4351-9. https://doi.org/10.1016/j.matpr.2019.07.395

- [7] Hada R, Goyal D, Singh Yadav V, Siddiqui N, Rani A. Synthesis of NiO nanoparticles loaded fly ash catalyst via microwave assisted solution combustion method and application in hydrogen peroxide decomposition. Mater Today Proc. 2020;28:119-23. https://doi.org/10.1016/j.matpr.2020.01.411
- [8] Yadav VK, et al. A novel and efficient method for the synthesis of amorphous nanosilica from fly ash tiles. Mater Today Proc. 2019;26:701-5. https://doi.org/10.1016/j.matpr.2020.01.013
- [9] Alharbi YR, Abadel AA, Mayhoub OA, Kohail M. Effect of using available metakaoline and nano materials on the behavior of reactive powder concrete. Constr Build Mater. 2019;269. https://doi.org/10.1016/j.conbuildmat.2020.121344
- [10] Huang Q, Zheng W, Xiao X, Dong J, Wen J, Chang C. Effects of fly ash, phosphoric acid, and nano-silica on the properties of magnesium oxychloride cement. Ceram Int. 2021;47:34341-51. https://doi.org/10.1016/j.ceramint.2021.08.347
- [11] Liu H, Zhang Y, Tong R, Zhu Z, Lv Y. Effect of nanosilica on impermeability of cement-fly ash system. 2020. https://doi.org/10.1155/2020/1243074
- [12] Nazerigivi A, Najigivi A. Study on mechanical properties of ternary blended concrete containing two different sizes of nano-SiO2. Compos Part B Eng. 2019;167:20-4. https://doi.org/10.1016/j.compositesb.2018.11.136
- [13] Verma M. Evaluation survey of concrete composite using nano and micro silica materials for better properties. Mater Today Proc. 2021.
- [14] Phan VTA, Tran HB, Vo VT. Potential usage of fly ash and nano silica in cement mortar for a sustainable construction. Transp Res Procedia. 2025;85:135-42. https://doi.org/10.1016/j.trpro.2025.03.143
- [15] Garg R, Garg R, Bansal M, Aggarwal Y. Experimental study on strength and microstructure of mortar in presence of micro and nano-silica. Mater Today Proc. 2020;43:769-77. https://doi.org/10.1016/j.matpr.2020.06.167
- [16] Reddy AN, Reddy GGK, Reddy PN, Reddy KS, Kavyateja BV. Analyzing the impact of nano-sized silica on composite concrete: A static approach utilizing response surface method. Res Eng Struct Mater. 2024;11:165-78. https://doi.org/10.17515/resm2024.172ma0202rs
- [17] Daoust K, et al. Carbon nanofibers encapsulated by polyethylene glycol increase the mechanical properties and durability of OPC mortars. Constr Build Mater. 2024;447. https://doi.org/10.1016/j.conbuildmat.2024.137986
- [18] Zailani WWA, et al. Characterisation at the bonding zone between fly ash based geopolymer repair materials and ordinary Portland cement concrete. Materials (Basel). 2021;14:1-14. https://doi.org/10.3390/ma14010056
- [19] Imoisili PE, Jen T-C. Synthesis and characterization of amorphous nano silica from South African coal fly ash. Mater Today Proc. 2023. https://doi.org/10.1016/j.matpr.2023.06.077
- [20] Yadav VK, Fulekar MH. Advances in methods for recovery of ferrous. Ceramics. 2020;3:384-420. https://doi.org/10.3390/ceramics3030034
- [21] Zhang P, Sha D, Li Q, Zhao S, Ling Y. Effect of nano silica particles on impact resistance and durability of concrete containing coal fly ash. Nanomaterials. 2021;11. https://doi.org/10.3390/nano11051296
- [22] Setiawati M, Saggaff A, Saloma, Ngian SP. Effect of solution concentration, fly ash ratio, and aging time on the quality of nano-silica. Sci Technol Indones. 2025;10:622-7. https://doi.org/10.26554/sti.2025.10.2.622-627
- [23] Meftah N, Hani A, Merdas A. Extraction and physicochemical characterization of highly-pure amorphous silica nanoparticles from locally available dunes sand. Chem Africa. 2023;6:3039-48. https://doi.org/10.1007/s42250-023-00688-2
- [24] Yadav VK, Amari A, Wanale SG, Osman H, Fulekar MH. Synthesis of floral-shaped nanosilica from coal fly ash and its application for the remediation of heavy metals from fly ash aqueous solutions. Sustainability. 2024;15. https://doi.org/10.3390/su15032612
- [25] Bassyouni AEM, Saleh M. Utilization of chemically modified coal fly ash as cost-effective adsorbent for removal of hazardous organic wastes. Int J Environ Sci Technol. 2023;20:7589-602. https://doi.org/10.1007/s13762-022-04457-5
- [26] Raj SR, Arulraj GP, Anand N, Kanagaraj B, Lubloy E. Influence of nano-fly ash on mechanical properties, microstructure characteristics and sustainability analysis of alkali activated concrete. Dev Built Environ. 2024;17:1-24. https://doi.org/10.1016/j.dibe.2024.100352
- [27] Humad AM, Dakhil JD, Al-Mashhadi SA, Al-Khafaji Z, Mohammed ZA, Jabr SF. Improvements of mechanical and physical features of cement mortar by nano AL2O3 and CaCO3 as additives. Res. Eng. Struct. Mater., 2024; 10(3): 857-871. http://dx.doi.org/10.17515/resm2023.43me0806rs
- [28] Ngo VT, Quang T, Lam K, My T, Do D, Nguyen TC. Nano concrete aggregation with steel fibers: A problem to enhance the tensile strength of concrete. E3S Web Conf. 2019;135:03001. https://doi.org/10.1051/e3sconf/201913503001
- [29] Zinad OS, Csiha C. Improving sustainability of mortar by wood-ash and nano-SiO2. Case Stud Chem Environ Eng. 2024;9:1-5. https://doi.org/10.1016/j.cscee.2023.100597